



POTSDAM-INSTITUT FÜR
KLIMAFOLGENFORSCHUNG

Originally published as:

Pitsik, E., Frolov, N., Krämer, K.-H., Grubov, V., Maksimenko, V., Kurths, J., Hramov, A. (2020): Motor execution reduces EEG signals complexity: Recurrence quantification analysis study. - *Chaos*, 30, 2, 023111.

DOI: <https://doi.org/10.1063/1.5136246>

This article may be downloaded for personal use only. Any other use requires prior permission of the author and AIP Publishing.

Motor execution reduces EEG signals complexity: recurrence quantification analysis study

Elena Pitsik,¹ Nikita Frolov,^{1, a)} K. Hauke Kraemer,^{2, 3} Vadim Grubov,¹ Vladimir Maksimenko,¹ Jürgen Kurths,^{2, 4} and Alexander Hramov^{1, b)}

¹⁾Neuroscience and Cognitive Technology Laboratory, Center for Technologies in Robotics and Mechatronics Components, Innopolis University, 420500, Innopolis, The Republic of Tatarstan, Russia

²⁾Potsdam Institute for Climate Impact Research, 14473 Potsdam, Germany

³⁾Institute of Geosciences, University of Potsdam, 14476 Potsdam-Golm, Germany

⁴⁾Department of Physics, Humboldt University, 12489 Berlin, Germany

(Dated: 16 December 2019)

The development of new approaches to detect motor-related brain activity is key in many aspects of science, especially in brain-computer interface (BCI) applications. Even though some well-known features of motor-related electroencephalograms (EEGs) have been revealed using traditionally applied methods, they still lack a robust classification of motor-related patterns. Here we introduce new features of motor-related brain activity and uncover hidden mechanisms of the underlying neuronal dynamics by considering event-related desynchronization (ERD) of μ -rhythm in the sensorimotor cortex, i.e. tracking the decrease of the power spectral density in the corresponding frequency band. We hypothesize that motor-related ERD is associated with the suppression of random fluctuations of μ -band neuronal activity. This is due to a lowering of the number of active neuronal populations involved in the corresponding oscillation mode. In this case we expect more regular dynamics and a decrease in complexity of the EEG signal recorded over the sensorimotor cortex. In order to support this theses we apply measures of signal complexity by means of recurrence quantification analysis (RQA). In particular, we demonstrate that certain RQA quantifiers are very useful to detect the moment of movement onset and therefore are able to classify the laterality of executed movements.

The detection of the motor-related brain activity for non-invasive EEG-based brain-computer interfaces is an actively discussed topic in many areas of research. This is of special interest in context of neurorehabilitation and non-muscular control of remote devices using BCI-based techniques. Traditionally used methods for motor-related feature extraction, such as spatial filtering and time-frequency analysis, allow to associate motor actions with ERD of μ -band oscillations (8-13 Hz) over the sensorimotor cortex. However, these features, i.e. location of brain activity sources, amplitudes of spectral components, etc., are of strong inter- and intrasubject variability. Moreover, inherent nonstationarity and a poor signal-to-noise ratio of EEG signals strongly complicate the detection and classification of motor-related patterns in single trials. To find new features of the motor-related brain activity we explore EEG signals from the viewpoint of signal complexity. In particular, we put forward the hypothesis that μ -band ERD causes reduction of random fluctuations of neuronal activity, resulting in a more regular behavior of EEG signals during motor task accomplishments. With this goal in mind we apply RQA, a nonlinear method which describes the recurrence structure of a system by several quantifiers, in order to examine its complexity and uncover hidden underlying phenomena. Our findings show that certain RQA measures, namely determinism and recurrence time entropy, allow to reveal new features associated with neuronal activity complexity reduction. These measures are not only sensitive to the tran-

sitions from background to motor-related brain activity, but also very useful for distinguishing different types of motor actions (left/right limbs motion), which is valuable in the context of potential BCI applications.

I. INTRODUCTION

The study of motor-related brain activity is a challenging task at the intersection of neuroscience, medicine, nonlinear physics and engineering. This problem is closely related to the neurorehabilitation of post-stroke patients suffering motor and cognitive impairment¹. Another branch of actual research demanding brain motor-related activity decryption is a mental control of robotic systems, prosthetic devices and vehicles². Translating the recorded signals of brain activity into control commands, brain-computer interfaces (BCIs) can provide a communication channel between the human and the external device³⁻⁵.

Recently a considerable progress has been achieved in invasive BCIs for motor control. This is due to the principles of the invasive interfaces operation, which rely on the firing properties of individual neurons or small groups of neighboring neurons modulating their activity according to the motor tasks⁶. In this case motor-related neuronal activity patterns are pronounced and well reproduced, which allows to develop precise schemes for motor control^{5,7}. Despite the outstanding ability for an accurate detection and translation of brain motor commands, the application of invasive BCIs for daily purposes is extremely difficult since it requires complex brain surgery, which is performed in rare cases of urgent need.

On the contrary, noninvasive BCIs are easy to apply and

^{a)}Electronic mail: n.frolov@innopolis.ru

^{b)}Electronic mail: a.hramov@innopolis.ru

much more convenient in terms of usability. Among the variety of neuroimaging methods, electroencephalography (EEG) appears to be one of the most suitable for routine BCI applications⁸. A comprehensive review on the current state and future perspectives of sensorimotor EEG-based interfaces was given by Yuan and He⁹. Traditionally, methods of spatial filtering^{10,11}, machine learning^{12,13} and time-frequency analysis^{14,15} are the core algorithms for feature extraction in this context.

However, the detection and classification of motor-related patterns of brain activity using noninvasive techniques is much more complicated. The fact is that EEG simultaneously records electrical activity of a large group of neuronal populations located close to the measuring sensor¹⁶. Generally, distinct neuronal ensembles do not behave in coherency. Therefore, EEG signals represent a complex mixture of local neuronal activity components. The latter determines inherent critical properties of EEG signals, such as a poor signal-to-noise ratio and nonstationarity. Besides, a number of studies reported that traditional features of motor-related brain activity such as amplitudes of EEG signals, power spectral density, time-frequency and spatial features, basically show inter- and intrasubject variability^{15,17–19}. Hence, it is of high interest to find relevant features and methods that will withstand the discussed weaknesses of EEG recordings.

It is known, that motor tasks block ongoing activity in the μ -band (8–13 Hz) of a EEG record, i.e. event-related desynchronization (ERD) takes place¹⁴. Motor-related ERD implies a time-locked decrease in the number of active neurons involved in μ -oscillations²⁰. We hypothesize that this is equivalent to a suppression of spontaneous fluctuation of neuronal activity in the corresponding frequency band compared to the preceding background activity. Thus, we expect that motor-related neuronal dynamics should be reflected in EEG recordings by the signal's complexity reduction.

To explore this phenomena, we apply recurrence quantification analysis (RQA), which provides a rich number of relevant measures of complexity^{21,22}. RQA is a powerful tool for the analysis of biological signals, specifically heart rate variability^{23,24}, muscle activity^{25,26}, sleep^{27–29} and pathological EEGs^{30,31}. Early RQA studies that focused on EEG analysis demonstrated the ability of RQA measures to quantify N400 event-related potentials (ERPs) in single trials³², which emphasizes the robustness of the RQA approach in the context of the current study.

In summary, this work intends to find new features of motor-related brain activity with the focus on motor-related reduction of EEG signal's complexity in the μ -band. Here, we test our hypothesis on the upper limb motor execution tasks and apply RQA to quantify changes of signal complexity caused by the motor task accomplishment. We demonstrate that certain RQA quantifiers are sensitive to the transition from background to motor-related brain activity which, in turn, reveals differences between left and right upper limb movements.

The paper is organized as follows. Section II describes the details of our experimental study, the data pre-/postprocessing and briefly the RQA method. Section III is devoted to the

analysis of the time-dependent RQA measures and the inference of task vs. background differences along with differences between left and right limb movements. Finally, we summarize our results and discuss them in context of BCI development in Section IV.

II. METHODS

A. Participants

Participants were recruited among the employees and students of the Innopolis University. During the data preparation, we selected 10 subjects (7 male, 3 female) according to the following checklist: healthy, aged 18–33, right-handed, never participated in this or similar experiments before and having no history of brain tumors, trauma or stroke-related medical conditions. All the participants were pre-informed about the goals and design of the experiment. Experimental studies were performed in accordance with the Declaration of Helsinki and approved by the local research Ethics Committee of Innopolis University.

B. Data acquisition

EEG signals along with electromyograms (EMGs) from both hands were recorded using non-invasive EEG/EMG system “Encephalan-EEGR-19/26” (Medicom MTD company, Taganrog, Russian Federation). Electrocardiogram (ECG) and electro-oculogram (EOG) were also recorded for further removal of cardiac and eye-movement artifacts. All recorded signals were amplified and digitized at the sampling rate of 250 Hz. In order to record motor brain activity we used 9 EEG Ag/AgCl electrodes Fc3, Fcz, Fc4, C3, Cz, C4, Cp3, Cpz, Cp4 located over the motor cortex according to the international “10-10” system proposed by the American Electroencephalographic Society. To capture hand movements execution we placed 4 EMG electrodes as follows: 1 reference on the wrist and 1 on the forearm muscle for each hand.

C. Experimental setup

The session started with a 5-min recording of background brain activity, during which the participants were instructed to relax and listen to classical music. They were also instructed not to think about anything special and to make no hand movements. Then, each participant, during the active phase of the experiment, performed two types of motor actions according to the experimental protocol, i.e. movements for the left and right hands (Fig. 1A). Each hand movement implied squeezing the hand into a fist after the first signal, holding it down to the second signal and then relaxing. The time interval between the first and the second signals was randomly chosen for each motor task in the range 4–5 s and the time interval between the second signal of the current task and the first signal of the next task (resting period) was randomly chosen in

This is the author's peer reviewed, accepted manuscript. However, the online version of record will be different from this version once it has been copyedited and typeset.
PLEASE CITE THIS ARTICLE AS DOI: 10.1063/1.5136246

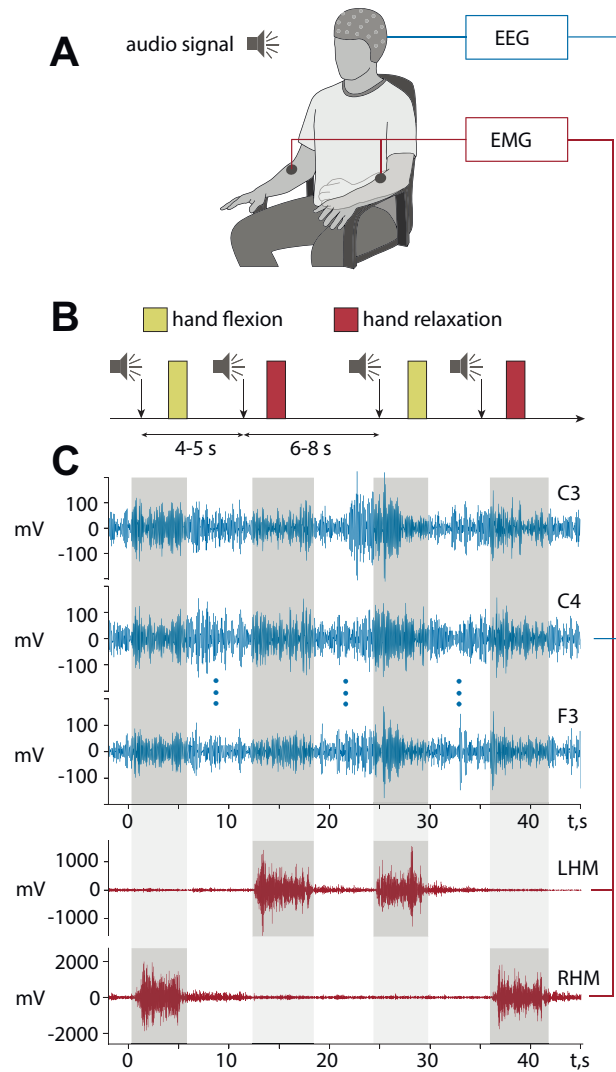


FIG. 1. **A** Schematic representation of the experimental procedure. Subjects were sitting comfortably in the chair while performing motor actions of left and right hands on audio signal command. **B** Experimental sequence. Time intervals between the signals were chosen randomly in ranges 4–5 seconds between first and second signals for one task and 6–8 seconds from second signal of previous and first signals of the next task. **C** Examples of recorded μ -band-pass filtered EEG and EMG signals (LHM = left hand movement, RHM = right hand movement).

the range 6–8 s (Fig. 1B). The active phase of the experiment consisted of 30 repetitions of each type of motor task (60 total) and the overall duration of the experimental procedure was approximately 18 minutes per participant, including background activity recording.

D. Data preprocessing

The following preprocessing steps were carried out to prepare raw EEG and EMG recordings for further analysis.

First, cardiac and eye-movement artifacts were removed using recorded ECG and EOG signals via artifact removal method based on Gram-Schmidt process³³. A Notch filter around 50 Hz was applied to EEG and EMG data to exclude power line effects.

Second, we applied a 5th-order Butterworth band-pass filter in the range 8–13 Hz to the 18 minute multichannel EEG signals in order to extract μ -band neuronal oscillations associated with motor-related brain activity. EMG recordings were also band-pass filtered (10–100 Hz) to capture pronounced high-frequency fluctuations of muscle activity caused by muscle tension during movement execution (Fig. 1C). The latter allows to determine exact times for the beginning and the end of movement executions and to study the motor-related brain activity at these specific intervals.

Finally, the bandpass filtered time series (both EEG and EMG) were split into 60 trials, each lasting 18 seconds (6 seconds before and 12 seconds after the command, totaling 4500 data points), i.e. 30 attempts for the left and right hand.

The considered EEG trials represent 9-dimensional multivariate sets $\mathbf{X}(t) = (x_{Cp4}(t), x_{C4}(t), x_{Fc4}(t), x_{Cpz}(t), x_{Cz}(t), x_{Fcz}(t), x_{Cp3}(t), x_{C3}(t), x_{Fc3}(t))^T$ composed of EEG signals recorded over the sensorimotor brain area (Fig. 2A). To describe brain dynamics in three areas of interest we separated \mathbf{X} into three 3D subsets, according to their location on the scalp (Fig. 2B):

1. **right hemisphere (RH):** $\mathbf{X}_L(t) = (x_{Cp4}(t), x_{C4}(t), x_{Fc4}(t))^T$;
2. **left hemisphere (LH):** $\mathbf{X}_R(t) = (x_{Cp3}(t), x_{C3}(t), x_{Fc3}(t))^T$;
3. **longitudinal fissure (F):** $\mathbf{X}_F(t) = (x_{Cpz}(t), x_{Cz}(t), x_{Fcz}(t))^T$.

Consequently, from a physical perspective, each brain area is represented by a three dimensional trajectory, treating the constitutive time series as state variables (Fig. 2C). This way of state space trajectory construction is convenient in the context of multivariate EEG analysis and circumvents the single variable embedding problem^{34–37}.

Of particular note is the fact that the further analysis deals with sensor-level EEG recordings. This is done to exclude EEG pre-processing steps related with source reconstruction and capture general effects of motor-related activity from the viewpoint of an overall decrease of complexity of the underlying neuronal processes in the sensorimotor cortex. The advantages and limitations of such approach will be discussed in Section III.

E. Recurrence quantification analysis

Being a fundamental property of most dynamical systems, recurrence implies that the system's state repeats itself in time³⁸. It is represented as neighboring points (states) of the system's trajectory in its state space. A common way of visualizing the system's repeating states is the recurrence plot

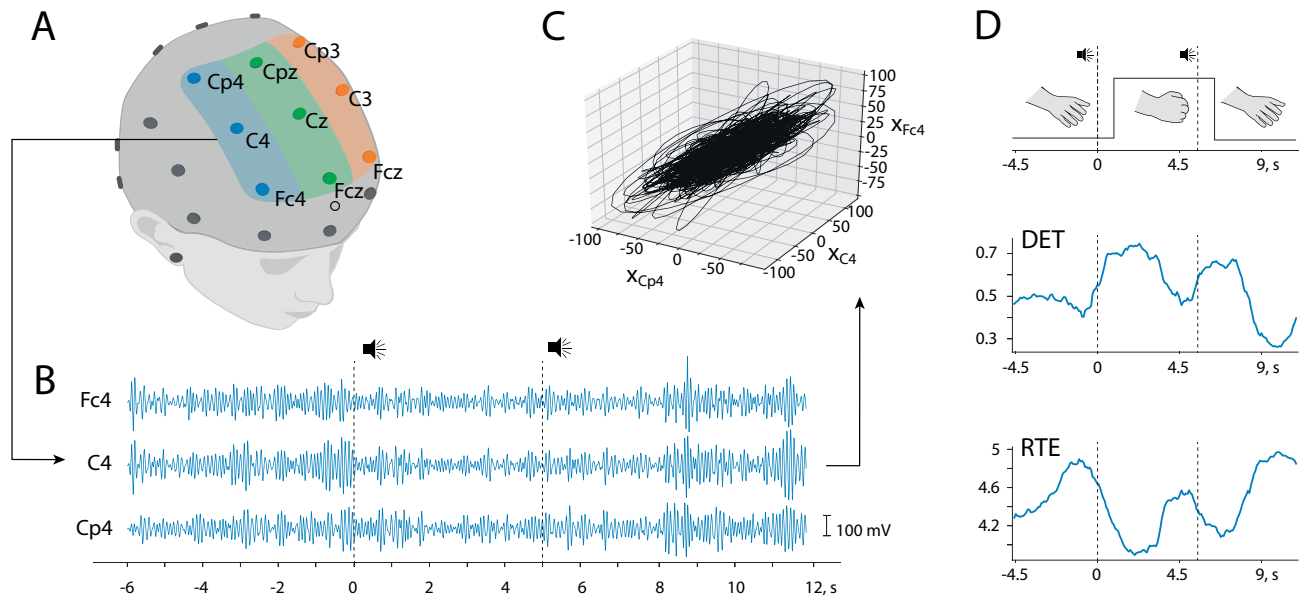


FIG. 2. Step-by-step visualization of the EEG signal analysis. **A** EEG electrodes, located at the sensorimotor area, forming a multivariate set $\mathbf{X}(t)$: right hemisphere (subset $\mathbf{X}_R(t)$, blue area), left hemisphere (subset $\mathbf{X}_L(t)$, orange area), and longitudinal fissure (subset $\mathbf{X}_F(t)$, green area). **B** Example of a motor-related EEG trial from $\mathbf{X}_R(t)$ (left hand movement). Vertical dashed lines correspond to the first and second audio signal at 0 s and 5 s, respectively. **C** Representation of the current trial from $\mathbf{X}_R(t)$ as a trajectory in 3D phase space. **D** Illustrative scheme of the movement execution accessed from a EMG signal (top panel) and corresponding time-dependent measures of *DET* (middle panel) and *RTE* (bottom panel).

(RP), which can show structures such as diagonal and horizontal/vertical lines and areas of different recurrence densities²¹. Certain structures are related to the system's complexity and recurrence quantification analysis (RQA) was introduced to analyze them numerically, using various measures of complexity²².

To analyze the recurrence structures in the selected brain areas, using the multivariate set X (Sect. IID), we created a binary recurrence matrix

$$R_{i,j} = \begin{cases} 1, & \text{if } (\varepsilon - \|\mathbf{X}_i - \mathbf{X}_j\|) < 0, \\ 0, & \text{otherwise} \end{cases} \quad (1)$$

where $\mathbf{X}_{i,j} = \mathbf{X}(t_{i,j})$, $i, j = 1, \dots, N$ with $N = 4500$ for the number of considered states \mathbf{X}_i . The recurrence threshold ε determines the size of the neighbourhood in state space in which states being considered as recurring²¹. When analyzing an RP one should take into account that the obtained results can crucially depend on the choice of this threshold. To provide a robust representation of the RP and ensuring comparability within the samples, i.e. data from different participants, we determined the value of the threshold ε for each sample as the 3rd percentile of the pairwise distance distribution, following Kraemer *et al.*³⁹,

To access time-dependence of the estimated RQA quantifiers we used a running window along the main diagonal line of each RP with a window size of $w = 750$ data points (3 s) and a shift $\delta w = 20$ data points (0.08 s).

In the current study we want to quantify regularity and complexity of EEG signals affected by motor tasks execution. Therefore we pick two suitable RQA quantifiers, namely the Determinism (*DET*) and the recurrence time entropy (*RTE*). *DET* is defined as the ratio of recurrence points that form diagonal lines to all recurrence points found in the RP:

$$DET = \frac{\sum_{l=l_{min}}^w IP(l)}{\sum_{l=1}^w IP(l)}, \quad (2)$$

where $P(l)$ is the histogram of diagonal lines l in the RP and $l_{min} = 2$ is the minimal considered length of a diagonal line. The presence of diagonal lines in the RP is an important indicator of a deterministic process, since in this case, trajectories at different points in time evolve in a similar manner. More correlated and regularized processes are characterized by longer diagonal lines and less isolated points.

Along with *DET*, we estimate the recurrence time entropy (*RTE*) – a complexity measure based on the “white” (non-recurrent) vertical lines indicating recurrence times t_w :

$$RTE = - \sum_{t_w=1}^{T_{max}} p(t_w) \ln p(t_w), \quad (3)$$

where $p(t_w) = h(t_w) / \sum_{t_w} h(t_w)$ is the estimated probability of a recurrence time t_w and $h(t_w)$ is the histogram of recurrence times obtained from the RP. This RQA measure is well suited for capturing the transitions between periodic and

chaotic dynamics (and vice versa), because it is related to the Kolmogorov-Sinai entropy⁴⁰. A regular process results in low RTE values, with a chaotic process increasing the number of different recurrence times, thus increasing its distribution $h(t_w)$ and consequently increasing the RTE value.

Typical single trial time series of DET and RTE are shown in Fig 2D. One can see the increase of DET and the decrease of RTE associated with two motor actions respectively following the corresponding audio signal. A detailed discussion of RQA results will be given based on the between-subject analysis in section III. For each participant, we average the RQA time series over the trials and exclude the baseline level (3 s prior the first audio signal):

$$\begin{aligned}\Delta DET(t) &= DET(t) - DET_{bckg}, \\ \Delta RTE(t) &= RTE(t) - RTE_{bckg},\end{aligned}\quad (4)$$

where DET_{bckg} and RTE_{bckg} are mean values of DET and RTE 3 s prior the first audio signal.

All RQA related computations were performed using the DynamicalSystems software library for Julia programming language⁴¹.

F. Statistical test

The motor-related changes of the RQA measures calculated at the different (area, time)-pairs are treated as different aspects of the data with respect to which the experimental conditions (motor-task vs baseline and left vs right limb movement) will be compared. Each (area, time)-pair is tested via statistical t-test. Since we do not know exactly the locus of the possible differences in the (area,time)-domain, the multiple comparisons problem (MCP) takes place. To control family-wise error rate (FWER) and address MCP we used nonparametric statistical test based on the random partitions following Maris and Oostenveld⁴².

III. RESULTS AND DISCUSSION

To address the main problem of the current study, namely the quantification of an expected reduction in the complexity and randomness of neuronal processes in the sensorimotor cortex in the execution of motor tasks, we consider general cross-subject effects of motor-related changes in the corresponding RQA time series. First, we analyze the transition from (random) background neuronal activity to brain activity in the accomplishment of motor tasks. Figure 3 shows the results of DET and RTE , averaged over the subjects and along with the standard error, for the movements of right (A, B) and left (C, D) hands. As noted in Section IID, we are particularly interested in differences in results regarding the right hemisphere (X_R , blue), the left hemisphere (X_L , orange) and the longitudinal fissure (X_F , green). These results indicate that motion execution is associated with an increase in DET (Fig. 3 A,C). In addition, DET takes local maxima near

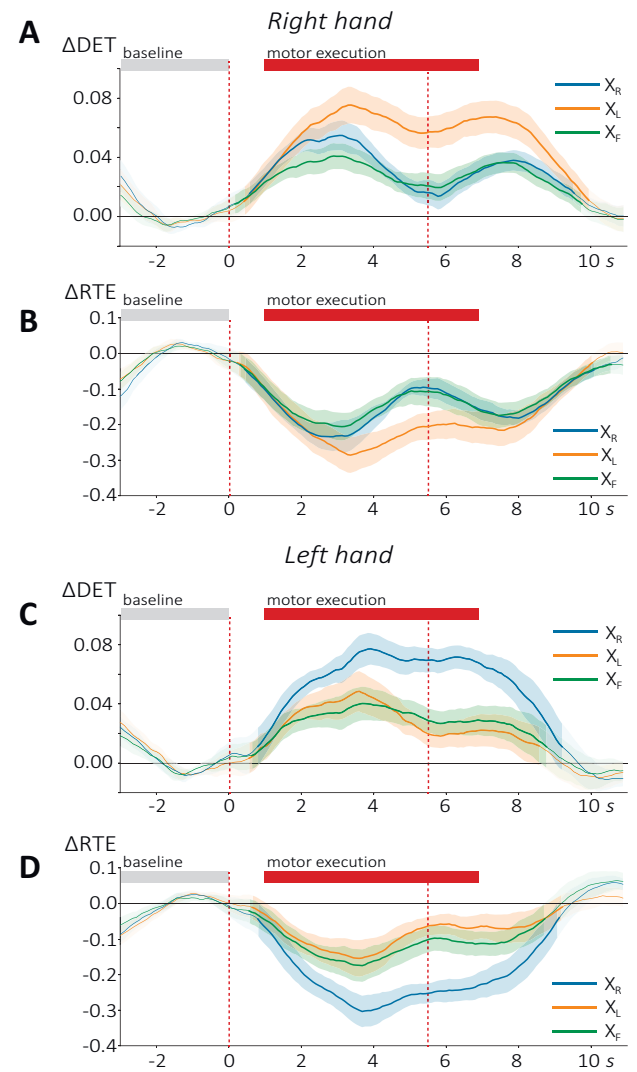


FIG. 3. Time dependence of ΔDET and ΔRTE averaged over all subjects ($\pm SE$) for the right hemisphere (X_R , blue), the left hemisphere (X_L , orange) and the longitudinal fissure (X_F , green) in case of the right (A, B) and left hand movements (C, D), respectively. Bold areas highlight the time intervals of significant divergence from the baseline level ($p < 0.05$, MCP corrected via a nonparametric statistical test). In each panel the red dashed lines indicate the moments of the first (0 s) and the second (5.5 s) audio signal and the black horizontal line corresponds to zero level. Gray boxes show 3 s baseline interval before the first audio signal and red boxes show the interval of movement execution obtained from averaged EMGs.

start (approximately 2–4 s after the first audio command) and end (approximately 7–8 s after the first command) of the motion execution. The positions of the local maxima are clearly associated with the hand flex and hand relaxation that are performed after the first and second audio commands, while the DET values decrease when holding the hands in a compressed state. The execution of motor tasks in this experimental setup is thus clearly characterized by the pronounced local increase of DET . In fact, the growth of DET implies a predictable or

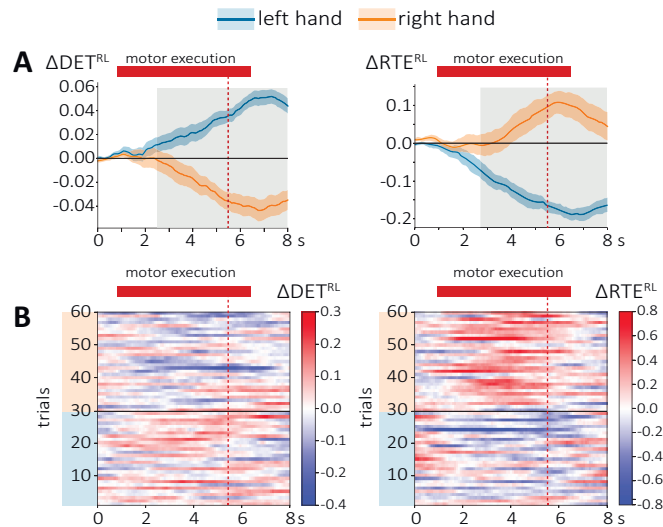


FIG. 4. **A** Time dependence of ΔDET^{RL} and ΔRTE^{RL} , derived from EEG data of the right and left hemispheres (Eq. (5), see text for details). Measures are averaged over the subjects and displayed as mean \pm SE. Shaded areas mark the areas with significant differences between the time series corresponding to left and right hand movements ($p < 0.05$, MCP corrected via nonparametric statistical test) and the red boxes indicate the movement execution interval determined from averaged EMGs. **B** Exemplary representation of motor-related EEG samples analysis on an individual test level using ΔDET^{RL} and ΔRTE^{RL} . EEG experiments are arranged as follows: left-hand movements (trials 1-30, highlighted in blue) and right-hand movements (trials 31-60, highlighted in orange).

regular motor neuronal activity. This finding is consistent with our hypothesis that motor action is associated with the suppression of random μ -band fluctuations in the EEG that are inherent in background activity. Local peaks of DET are accompanied by a decrease of RTE (Fig. 3 B,D). This also shows that the underlying motor neuronal activity recorded by the EEG becomes less chaotic and complex. A non-parametric statistical test in the (area,time)-domain (cf. Sect. II F) shows that the described motor changes of the RQA quantifiers compared to the background activity are significant ($p < 0.05$) for all three considered areas during the duration of the motor task execution. The occurrence of significant changes about 1.5 s before and after the execution of the motor task is related to the half width of the selected window size $w = 3$ s. It is noteworthy that the RQA measurements return to the background level after the end of the movement, which is a clear indication of the backward transition of the neuronal dynamics into the background mode.

It should be noted that the RQA time series for the right and left hands have a similar qualitative time course (two maxima/minima associated with hand flexion and relaxation) but assume involvement of the different brain areas. Particularly, right hand movement reduces the complexity of neural dynamics in the left hemisphere more (orange curve in Fig. 3 A,B) and the left hand movement – in the right hemi-

sphere (blue curve in Fig. 3 C,D). It coincides with the known contralaterality of the brain's motor-related activity. However, complexity reduction in the ipsilateral brain area and fissure region, even being not such pronounced, is also observed during the movement execution. This could be due to the volume conduction/field spread effect, which is critical for non-invasive measurements⁴³. Despite these limitations, analyzing the complexity of neuronal dynamics using RQA makes it possible to distinguish between the further discussed lateral types of motor actions.

Let us take a closer look at the differences in brain dynamics during right and left hand movements with respect to contralateral effects. For further analysis we only use the \mathbf{X}_R and \mathbf{X}_L records and introduce a measure of asymmetry as the differences between RQA measures in the right and left hemisphere for both hands:

$$\begin{aligned}\Delta DET^{RL}(t) &= \Delta DET^R(t) - \Delta DET^L(t) \\ \Delta RTE^{RL}(t) &= \Delta RTE^R(t) - \Delta RTE^L(t)\end{aligned}\quad (5)$$

where superscripts R and L indicate right and left hemispheres, respectively. Figure 4 A shows the course of $\Delta DET^{RL}(t)$ and $\Delta RTE^{RL}(t)$ during the motion execution, averaged over all subjects and along with the standard error. Here, the first audio signal corresponds to the time $t = 0$. In addition to the previous results, Fig. 4 shows that the reduction of the complexity of the neural dynamics during the execution of left and right hand movements **takes place in a different way**. A comparison of ΔDET^{RL} and ΔRTE^{RL} for left- and right-hand movements using a nonparametric statistical test shows that both measures reflect significant differences between the types of movement. **Specifically, reducing the complexity of the underlying neuronal dynamics results in pronounced interlateral asymmetry during movement execution, which is reflected in a maximum at DET and a minimum at RTE in case of the left hand movement and vice versa for the right.** Note that the asymmetry measures based on both DET and RTE , show significant differences of right- and left-hand motion (Fig. 4A). The introduced measures discriminate the brain dynamics associated with left and right hand movement may based on a statistical test (cf. Sect. II F) at an interval that approximately covers the motion execution (2.5–8 s after the first audio signal). In fact, the disclosed properties of motor-related EEG samples associated with contralateral asymmetry are suitable for a single-trial analysis and classification. Figure 4 B shows the exemplary representation of RQA applied to individual EEG experiments collected from a randomly selected subject. It can be seen, that the chosen RQA quantifiers are able to clearly distinguish between left- and right-hand movements: the former are characterized by the positive $\Delta DET^{RL}(t)$ and simultaneously negative $\Delta RTE^{RL}(t)$ values and vice versa for the latter.

In summary, we would like to emphasize that the discussed features of motor neuronal activity detected by EEG signals at the sensor level through RQA complexity measurements are clearly observed and well reproduced in the experimental group under consideration. What is more important is that

the generality of the cross-subject analysis provided also applies to the single trial analysis (see exemplary illustration in Fig. 2E). The latter, together with the low computational cost of RQA algorithms, offers the prospect of their application in EEG-based BCIs for motion control and assessment. However, the implementation of the RQA methods for stable operation in real-time detection and classification of motor-related brain states requires additional extensive research.

IV. CONCLUSION

We have used RQA to study new features of motor-related neuronal processes that are measured by non-invasive EEG. In our analysis, we have focused on the consideration of time-dependent RQA quantifiers based on diagonal lines (determinism, *DET*) and non-recurrent vertical lines (recurrence time entropy, *RTE*). These measures are suitable for detecting transitions between regular (periodic) and irregular (chaotic) dynamics and for quantifying the complexity of the system under study. Both quantifiers clearly show that the direct execution of motor tasks is associated with a large increase in the regularity of the EEG signals, i.e. a reduction in the complexity of underlying motor-related neuronal processes. In other words, RQA has shown that μ -band ERD causes a reduction in random fluctuations in neuronal activity inherent in background brain activity, leading to more regular behavior of the EEG signal during motor task execution. In addition to detecting an increase in motor-related regularity of brain dynamics, *DET* and *RTE* measurements are sensitive enough to indicate the difference between two lateral types of motion due to the inherent differences in neuronal response. **Specifically, we observed a strong increase in regularity in the sensorimotor area contralateral to the executed movement. Despite the limitations of EEG analysis at the sensor level, such as volume conduction/field spreading effect, interhemispheric asymmetry the *DET* and *RTE* values, which also supported statistically significant differences between two types of performed movements.**

Overall, the current results are consistent with and complement the well known concepts of motor-related brain processes. We suppose that the discovered features of neuronal dynamics in the sensorimotor cortex and the robust RQA methods of identification and classification will contribute to the study of non-invasive EEG-based BCI development for motor control and rehabilitation^{5,44–46}.

ACKNOWLEDGMENTS

The work has been supported by Russian Science Foundation (Grant No. 17-72-30003). The Authors gratefully acknowledge Dr. Bedartha Goswami and Dr. Norbert Marwan for the valuable discussions.

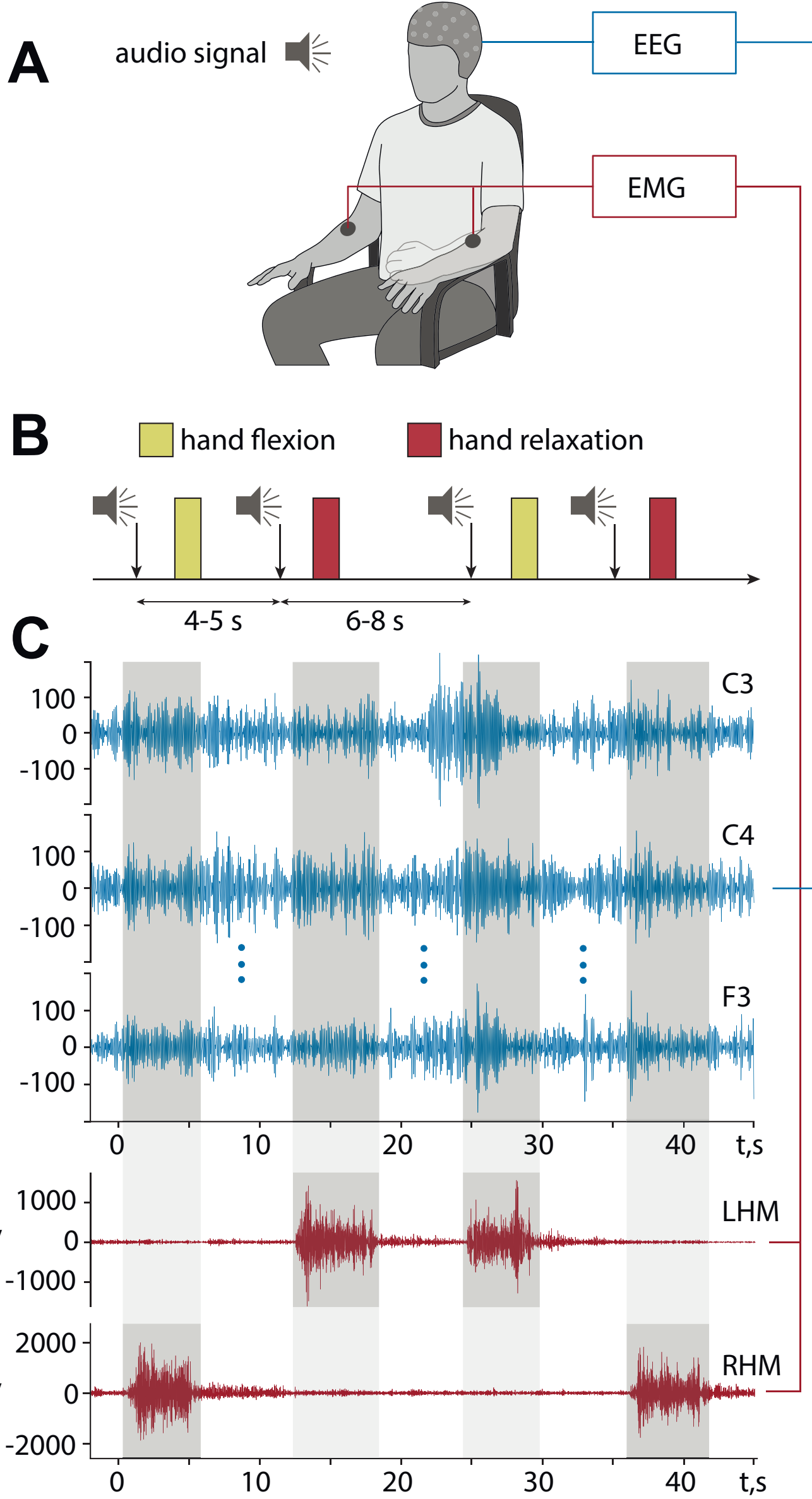
- ¹M. E. Stoykov and S. Madhavan, “Motor priming in neurorehabilitation,” *Journal of neurologic physical therapy: JNPT* **39**, 33 (2015).
²D. J. McFarland and J. R. Wolpaw, “Brain-computer interface operation of robotic and prosthetic devices,” *Computer* **41**, 52–56 (2008).

- ³J. R. Wolpaw, N. Birbaumer, D. J. McFarland, G. Pfurtscheller, and T. M. Vaughan, “Brain-computer interfaces for communication and control,” *Clinical neurophysiology* **113**, 767–791 (2002).
⁴U. Chaudhary, N. Birbaumer, and A. Ramos-Murguialday, “Brain-computer interfaces for communication and rehabilitation,” *Nature Reviews Neurology* **12**, 513 (2016).
⁵M. A. Lebedev and M. A. Nicolelis, “Brain-machine interfaces: From basic science to neuroprostheses and neurorehabilitation,” *Physiological reviews* **97**, 767–837 (2017).
⁶M. A. Lebedev and M. A. Nicolelis, “Brain-machine interfaces: past, present and future,” *TRENDS in Neurosciences* **29**, 536–546 (2006).
⁷A. L. Benabid, T. Costecalde, A. Eliseyev, G. Charvet, A. Verney, S. Karakas, M. Foerster, A. Lambert, B. Morinière, N. Abroug, *et al.*, “An exoskeleton controlled by an epidural wireless brain-machine interface in a tetraplegic patient: a proof-of-concept demonstration,” *The Lancet Neurology* (2019).
⁸D. McFarland and J. Wolpaw, “Eeg-based brain-computer interfaces,” *current opinion in Biomedical Engineering* **4**, 194–200 (2017).
⁹H. Yuan and B. He, “Brain-computer interfaces using sensorimotor rhythms: current state and future perspectives,” *IEEE Transactions on Biomedical Engineering* **61**, 1425–1435 (2014).
¹⁰H. Ramoser, J. Muller-Gerking, and G. Pfurtscheller, “Optimal spatial filtering of single trial eeg during imagined hand movement,” *IEEE transactions on rehabilitation engineering* **8**, 441–446 (2000).
¹¹C. Brunner, M. Naeem, R. Leeb, B. Graimann, and G. Pfurtscheller, “Spatial filtering and selection of optimized components in four class motor imagery eeg data using independent components analysis,” *Pattern recognition letters* **28**, 957–964 (2007).
¹²V. A. Maksimenko, S. A. Kurkin, E. N. Pitsik, V. Y. Musatov, A. E. Runnova, T. Y. Efremova, A. E. Hramov, and A. N. Pisarchik, “Artificial neural network classification of motor-related eeg: An increase in classification accuracy by reducing signal complexity,” *Complexity* **2018** (2018).
¹³P. Chholak, G. Niso, V. A. Maksimenko, S. A. Kurkin, N. S. Frolov, E. N. Pitsik, A. E. Hramov, and A. N. Pisarchik, “Visual and kinesthetic modes affect motor imagery classification in untrained subjects,” *Scientific reports* **9**, 1–12 (2019).
¹⁴G. Pfurtscheller, C. Brunner, A. Schlögl, and F. L. Da Silva, “Mu rhythm (de) synchronization and eeg single-trial classification of different motor imagery tasks,” *NeuroImage* **31**, 153–159 (2006).
¹⁵V. A. Maksimenko, A. Pavlov, A. E. Runnova, V. Nedaivozov, V. Grubov, A. Koronovskii, S. V. Pchelintseva, E. Pitsik, A. N. Pisarchik, and A. E. Hramov, “Nonlinear analysis of brain activity, associated with motor action and motor imagery in untrained subjects,” *Nonlinear Dynamics* **91**, 2803–2817 (2018).
¹⁶V. A. Maksimenko, A. Lüttjohann, V. V. Makarov, M. V. Goremyko, A. A. Koronovskii, V. Nedaivozov, A. E. Runnova, G. van Luijtelea, A. E. Hramov, and S. Boccaletti, “Macroscopic and microscopic spectral properties of brain networks during local and global synchronization,” *Physical Review E* **96**, 012316 (2017).
¹⁷T.-E. Kam, H.-I. Suk, and S.-W. Lee, “Non-homogeneous spatial filter optimization for electroencephalogram (eeg)-based motor imagery classification,” *Neurocomputing* **108**, 58–68 (2013).
¹⁸J. Asensio-Cubero, J. Gan, and R. Palaniappan, “Multiresolution analysis over simple graphs for brain computer interfaces,” *Journal of neural engineering* **10**, 046014 (2013).
¹⁹V. Grubov, V. Y. Musatov, V. Maksimenko, A. Pisarchik, A. Runnova, and A. Hramov, “Development of intelligent system for classification of multiple human brain states corresponding to different real and imaginary movements,” *Cybernetics and Physics* **6**, 103–107 (2017).
²⁰G. Pfurtscheller and F. L. Da Silva, “Event-related eeg/meg synchronization and desynchronization: basic principles,” *Clinical neurophysiology* **110**, 1842–1857 (1999).
²¹N. Marwan, M. C. Romano, M. Thiel, and J. Kurths, “Recurrence plots for the analysis of complex systems,” *Physics reports* **438**, 237–329 (2007).
²²C. L. Webber Jr and N. Marwan, “Recurrence quantification analysis,” *Theory and Best Practices* (2015).
²³N. Marwan, N. Wessel, U. Meyerfeldt, A. Schirdewan, and J. Kurths, “Recurrence-plot-based measures of complexity and their application to heart-rate-variability data,” *Physical review E* **66**, 026702 (2002).
²⁴U. R. Acharya, E. C.-P. Chua, O. Faust, T.-C. Lim, and L. F. B. Lim,

This is the author's peer reviewed, accepted manuscript. However, the online version of record will be different from this version once it has been copyedited and typeset.
PLEASE CITE THIS ARTICLE AS DOI: 10.1063/1.5136246

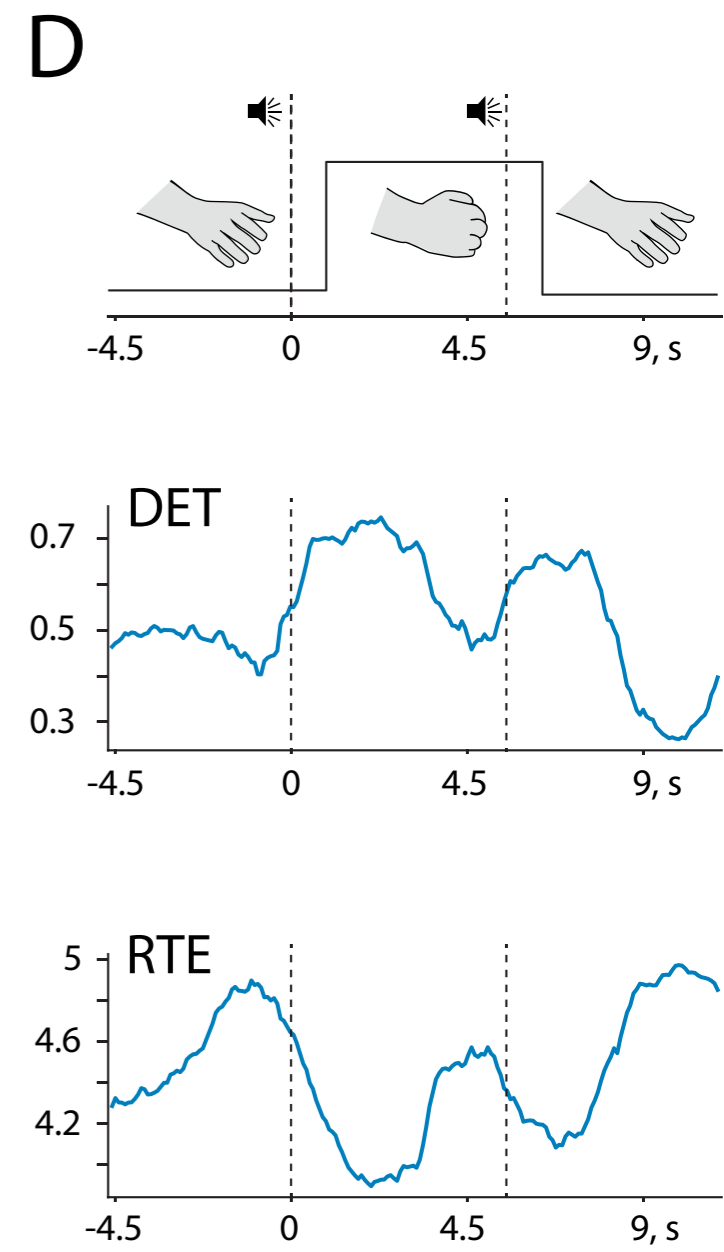
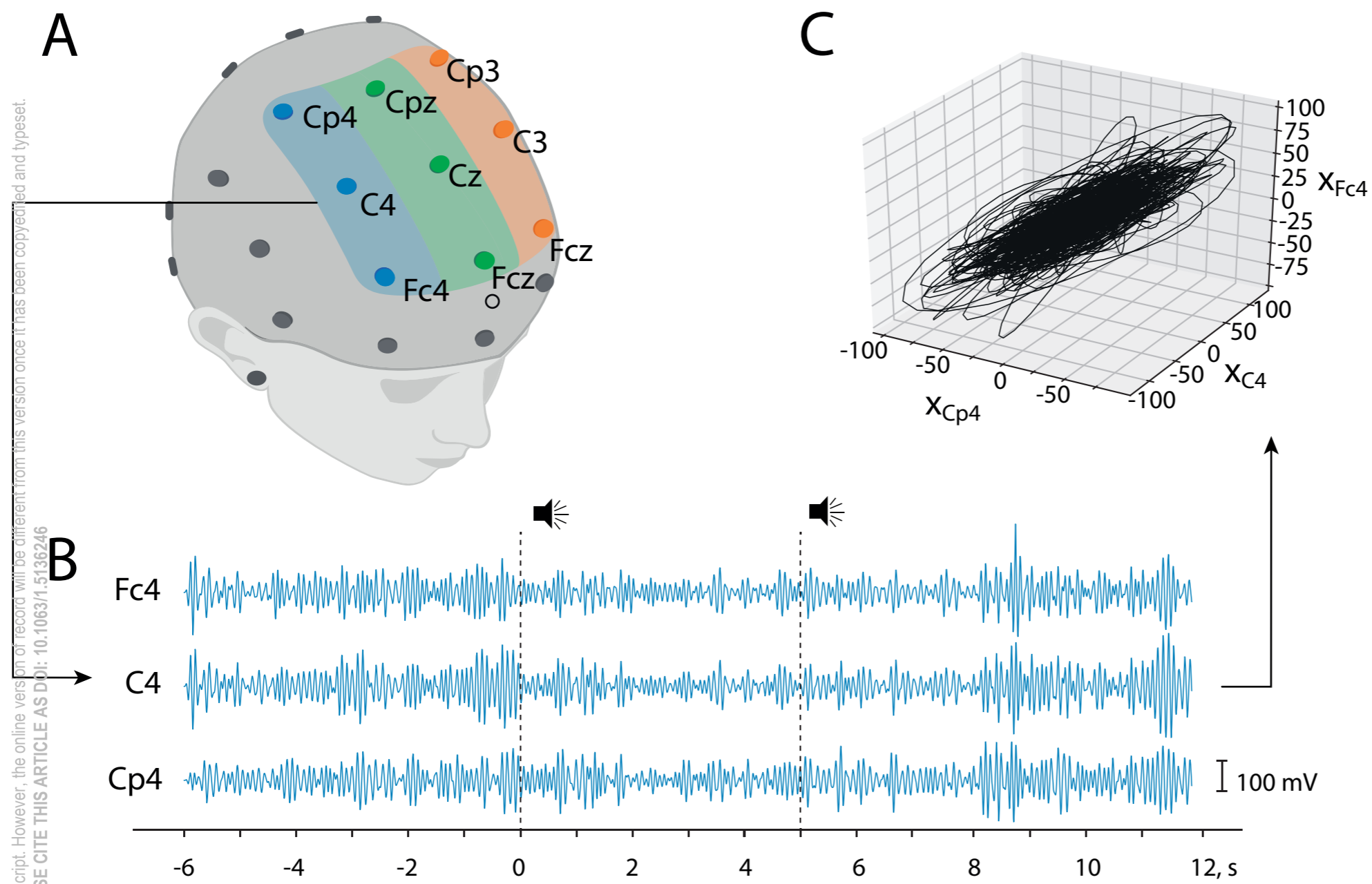
- "Automated detection of sleep apnea from electrocardiogram signals using nonlinear parameters," *Physiological measurement* **32**, 287 (2011).
- ²⁵S. Ikegawa, M. Shinohara, T. Fukunaga, J. P. Zbilut, and C. L. Webber Jr, "Nonlinear time-course of lumbar muscle fatigue using recurrence quantifications," *Biological cybernetics* **82**, 373–382 (2000).
- ²⁶C. Bauer, F. Rast, M. Ernst, A. Meichtry, J. Kool, S. Rissanen, J. Suni, and M. Kankaanpää, "The effect of muscle fatigue and low back pain on lumbar movement variability and complexity," *Journal of Electromyography and Kinesiology* **33**, 94–102 (2017).
- ²⁷U. R. Acharya, S. Bhat, O. Faust, H. Adeli, E. C.-P. Chua, W. J. E. Lim, and J. E. W. Koh, "Nonlinear dynamics measures for automated eeg-based sleep stage detection," *European neurology* **74**, 268–287 (2015).
- ²⁸G. Z. dos Santos Lima, S. R. Lopes, T. L. Prado, B. Lobao-Soares, G. C. do Nascimento, J. Fontenele-Araujo, and G. Corso, "Predictability of arousal in mouse slow wave sleep by accelerometer data," *PloS one* **12**, e0176761 (2017).
- ²⁹V. Parro and L. Valdo, "Sleep-wake detection using recurrence quantification analysis," *Chaos: An Interdisciplinary Journal of Nonlinear Science* **28**, 085706 (2018).
- ³⁰E. J. Ngamga, S. Bialonski, N. Marwan, J. Kurths, C. Geier, and K. Lehnertz, "Evaluation of selected recurrence measures in discriminating preictal and inter-ictal periods from epileptic eeg data," *Physics Letters A* **380**, 1419–1425 (2016).
- ³¹T. Rings, M. Mazarei, A. Akhshi, C. Geier, M. R. R. Tabar, and K. Lehnertz, "Traceability and dynamical resistance of precursor of extreme events," *Scientific reports* **9**, 1744 (2019).
- ³²N. Marwan and A. Meinke, "Extended recurrence plot analysis and its application to erp data," *International Journal of Bifurcation and Chaos* **14**, 761–771 (2004).
- ³³A. E. Hramov, V. A. Maksimenko, S. V. Pchelintseva, A. E. Runnova, V. V. Grubov, V. Y. Musatov, M. O. Zhuravlev, A. A. Koronovskii, and A. N. Pisarchik, "Classifying the perceptual interpretations of a bistable image using eeg and artificial neural networks," *Frontiers in neuroscience* **11**, 674 (2017).
- ³⁴C. Letellier, J. Maquet, L. L. Sceller, G. Gouesbet, and L. A. Aguirre, "On the non-equivalence of observables in phase-space reconstructions from recorded time series," *Journal of Physics A: Mathematical and General* **31**, 7913–7927 (1998).
- ³⁵C. Letellier, I. M. Moroz, and R. Gilmore, "Comparison of tests for embeddings," *Phys. Rev. E* **78**, 026203 (2008).
- ³⁶C. J. Cellucci, A. M. Albano, and P. E. Rapp, "Comparative study of embedding methods," *Phys. Rev. E* **67**, 066210 (2003).
- ³⁷K. Judd and A. Mees, "Embedding as a modeling problem," *Physica D: Nonlinear Phenomena* **120**, 273 – 286 (1998).
- ³⁸N. Marwan, "A historical review of recurrence plots," *The European Physical Journal Special Topics* **164**, 3–12 (2008).
- ³⁹K. H. Kraemer, R. V. Donner, J. Heitzig, and N. Marwan, "Recurrence threshold selection for obtaining robust recurrence characteristics in different embedding dimensions," *Chaos: An Interdisciplinary Journal of Nonlinear Science* **28**, 085720 (2018).
- ⁴⁰M. S. Baptista, E. J. Ngamga, P. R. F. Pinto, M. Brito, and J. Kurths, "Kolmogorov-Sinai entropy from recurrence times," *Physics Letters A* **374**, 1135–1140 (2010).
- ⁴¹G. Datsis, "Dynamicalsystems.jl: A julia software library for chaos and nonlinear dynamics," *Journal of Open Source Software* **3**, 598 (2018).
- ⁴²E. Maris and R. Oostenveld, "Nonparametric statistical testing of eeg- and meg-data," *Journal of neuroscience methods* **164**, 177–190 (2007).
- ⁴³J.-M. Schoffelen and J. Gross, "Source connectivity analysis with meg and eeg," *Human brain mapping* **30**, 1857–1865 (2009).
- ⁴⁴T. Ma, H. Li, L. Deng, H. Yang, X. Lv, P. Li, F. Li, R. Zhang, T. Liu, D. Yao, *et al.*, "The hybrid bci system for movement control by combining motor imagery and moving onset visual evoked potential," *Journal of neural engineering* **14**, 026015 (2017).
- ⁴⁵A. A. Frolov, O. Mokienko, R. Lyukmanov, E. Biryukova, S. Kotov, L. Turbina, G. Nadareyshvily, and Y. Bushkova, "Post-stroke rehabilitation training with a motor-imagery-based brain-computer interface (bci)-controlled hand exoskeleton: a randomized controlled multicenter trial," *Frontiers in neuroscience* **11**, 400 (2017).
- ⁴⁶A. R. Kiselev, V. A. Maksimenko, N. Shukovskiy, A. N. Pisarchik, E. Pit-sik, and A. E. Hramov, "Post-stroke rehabilitation with the help of brain-computer interface," in *2019 3rd School on Dynamics of Complex Networks and their Application in Intellectual Robotics (DCNAIR)* (IEEE, 2019) pp. 83–85.

This is the author's peer reviewed, accepted manuscript. However, the online version of record will be different from this version once it has been copyedited and typeset.
PLEASE CITE THIS ARTICLE AS DOI: 10.1063/1.5136246

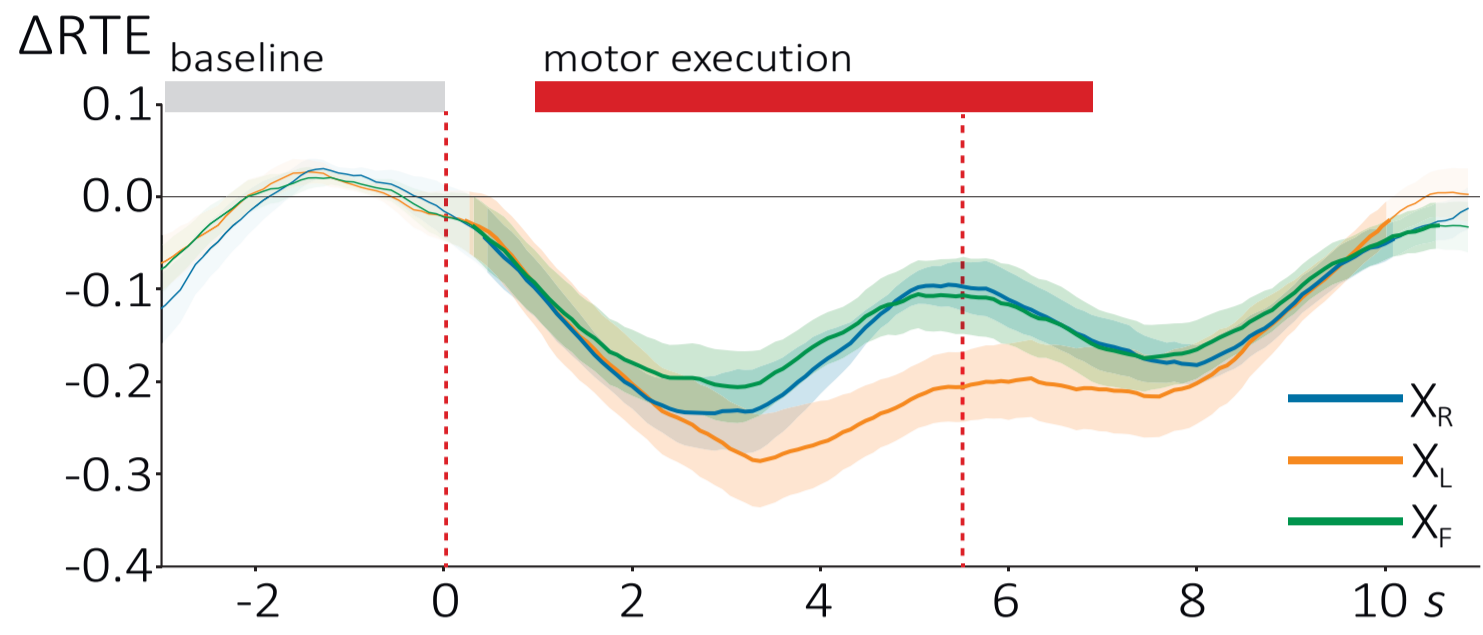
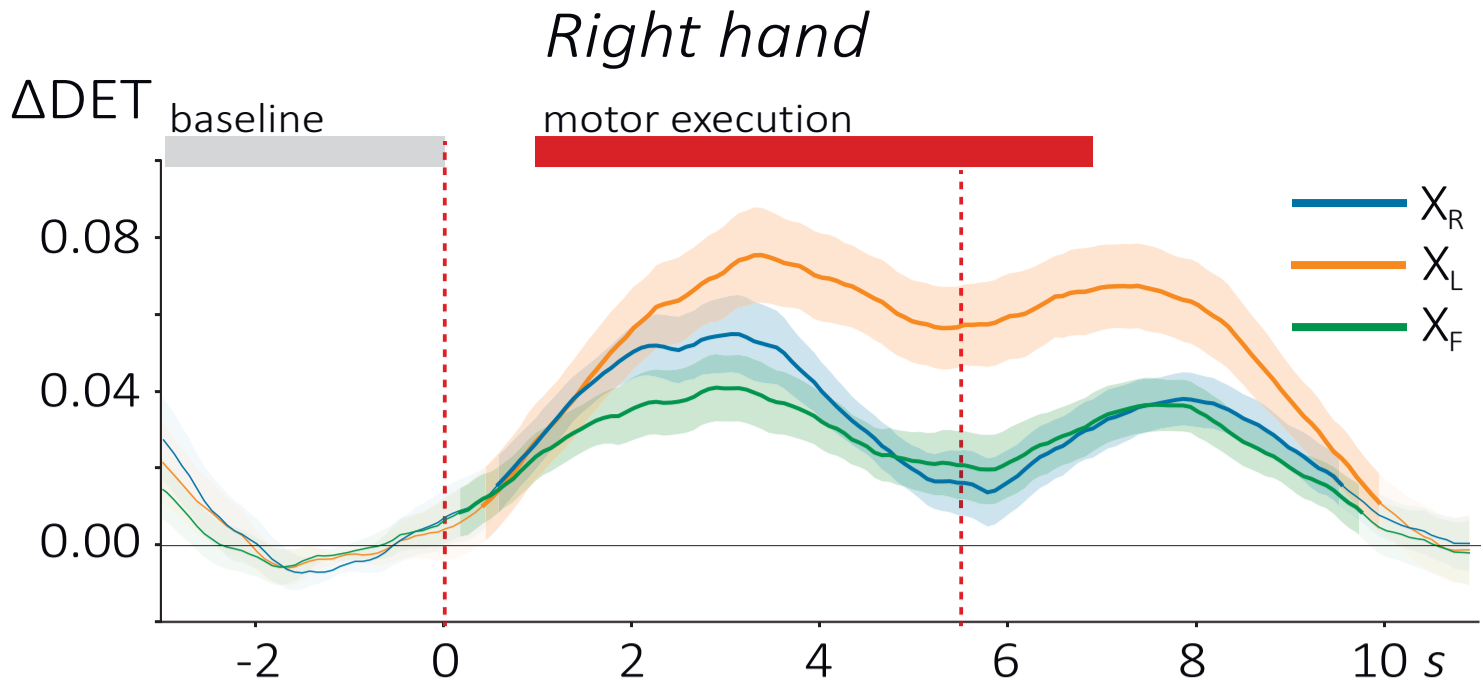
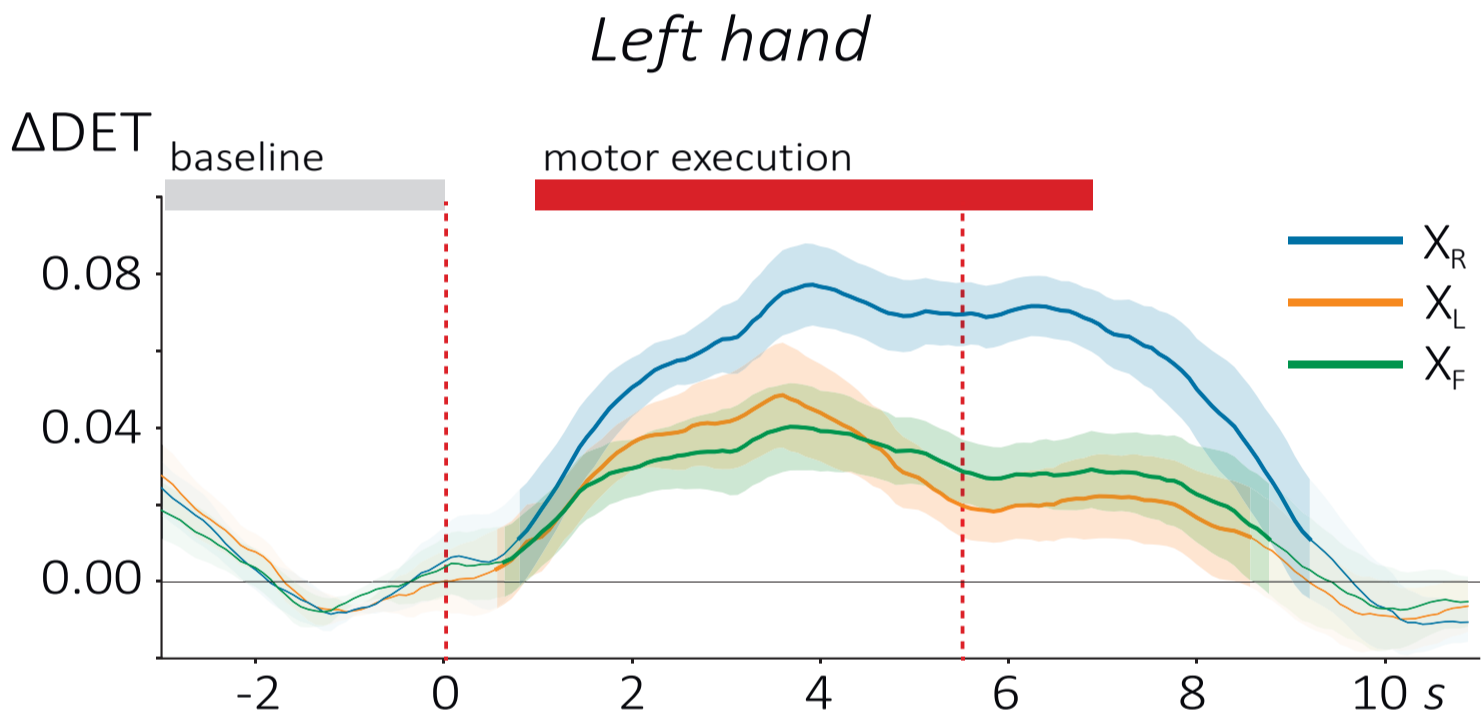
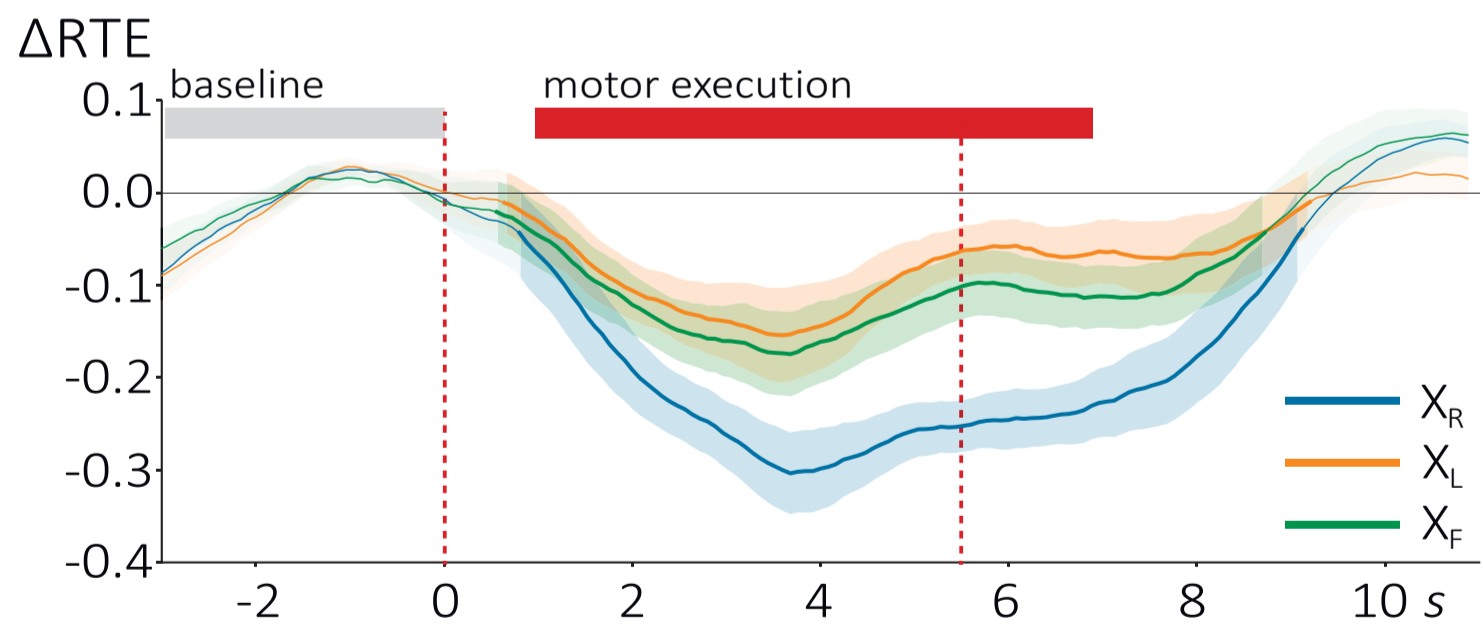


This is the author's peer reviewed, accepted manuscript. However, the online version of record will be different from this version once it has been copyedited and typeset.

PLEASE CITE THIS ARTICLE AS DOI: 10.1063/1.5136246



This is the author's peer-reviewed, accepted manuscript. However, the online version of record will be different from this version once it has been copyedited and typeset.
PLEASE CITE THIS ARTICLE AS DOI: 10.1063/1.5336246

A**B****C****D**

This is the author's peer reviewed, accepted manuscript. However, the online version of this record will be different from this version once it has been copyedited and typeset. PLEASE CITE THIS ARTICLE AS DOI:10.1063/1.5136246

A